

# Does regional air–sea coupling improve the simulation of the summer monsoon over the western North Pacific in the WRF4 model?

Liwei ZOU

To cite this article: Liwei ZOU (2020): Does regional air–sea coupling improve the simulation of the summer monsoon over the western North Pacific in the WRF4 model?, Atmospheric and Oceanic Science Letters, DOI: [10.1080/16742834.2020.1819755](https://doi.org/10.1080/16742834.2020.1819755)

To link to this article: <https://doi.org/10.1080/16742834.2020.1819755>



© 2020 The Author(s). Published by Informa UK Limited, trading as Taylor & Francis Group.



[View supplementary material](#)



Published online: 07 Oct 2020.



[Submit your article to this journal](#)



Article views: 48



[View related articles](#)



[View Crossmark data](#)

# Does regional air–sea coupling improve the simulation of the summer monsoon over the western North Pacific in the WRF4 model?

ZOU Liwei

State Key Laboratory of Numerical Modeling for Atmospheric Sciences and Geophysical Fluid Dynamics, Institute of Atmospheric Physics, Chinese Academy of Sciences, Beijing, China

## ABSTRACT

A new regional coupled ocean–atmosphere model, WRF4-LICOM, was used to investigate the impacts of regional air–sea coupling on the simulation of the western North Pacific summer monsoon (WNPSM), with a focus on the normal WNPSM year 2005. Compared to WRF4, WRF4-LICOM improved the simulation of the summer mean monsoon rainfall, circulations, sea surface net heat fluxes, and propagations of the daily rainband over the WNP. The major differences between the models were found over the northern South China Sea and east of the Philippines. The warmer SST reduced the gross moist stability of the atmosphere and increased the upward latent heat flux, and then drove local ascending anomalies, which led to the increase of rainfall in WRF4-LICOM. The resultant enhanced atmospheric heating drove a low-level anomalous cyclone to its northwest, which reduced the simulated circulation biases in the stand-alone WRF4 model. The local observed daily SST over the WNP was a response to the overlying summer monsoon. In the WRF4 model, the modeled atmosphere exhibited passive response to the underlying daily SST anomalies. With the inclusion of regional air–sea coupling, the simulated daily SST–rainfall relationship was significantly improved. WRF4-LICOM is recommended for future dynamical downscaling of simulations and projections over this region.

## ARTICLE HISTORY

Received 27 February 2020  
Revised 5 April 2020  
Accepted 13 April 2020

## KEYWORDS

Regional coupled ocean–atmosphere model; regional climate model; western North Pacific summer monsoon; regional air–sea interactions

## 关键词

区域海气耦合模式; 区域气候模式; 西北太平洋夏季风; 海气耦合过程

## 海气耦合过程改进了WRF4模式模拟的西北太平洋夏季风

### 摘要

利用新的区域海气耦合模式WRF4-LICOM研究了海气耦合过程对西北太平洋夏季风模拟的影响。研究表明, 耦合模式改进了非耦合模式模拟的西北太平洋夏季平均降水, 环流, 海表净热通量和夏季雨带的南北移动。耦合与非耦合模式的差异主要在南海北部及菲律宾岛以东地区。耦合模式里更暖的海温减弱了大气的总体湿稳定度, 增强了向上的潜热通量, 导致局地异常上升运动, 使得局地降水增加。进一步分析表明, 海气耦合过程明显改进了日平均SST-降水的相关关系。因此, 未来针对该区域气候变化模拟和预估动力降尺度建议采用区域耦合模式。


## 1. Introduction

Regional coupled ocean–atmosphere models, which include regional air–sea interactions and have relatively high horizontal resolution, have been widely developed for a broad range of applications, from regional climate process studies to climate change simulations (Zou and Zhou 2012; Giorgi 2019). Particular studies on regional coupled ocean–atmosphere models have focused on the Mediterranean domain (Ruti et al. 2016) and the monsoon regions, i.e., the West African monsoon (Hagos and Cook 2009), Indian monsoon (e.g., Ratnam et al. 2009), East Asian monsoon (e.g., Ren and Qian 2005), and Asian monsoon (Zou and Zhou 2016). Two flagship pilot studies on regional ocean–atmosphere–land interactions focused on western-southern Africa

and the Mediterranean region have been endorsed by the Coordinated Regional Downscaling Experiment (Gutowski et al. 2016) (<http://www.cordex.org/endorsed-flagship-pilot-studies/>).

One of the foci of research that employs a regional coupled ocean–atmosphere model is the Asian summer monsoon. Comparisons between coupled and uncoupled air–sea regional climate simulations show that coupled regional models tend to reduce the biases simulated by uncoupled regional climate models, especially with respect to the climatology and interannual variability of summer monsoon rainfall and circulations over the Indian monsoon region (Ratnam et al. 2009), East Asian monsoon region (Li and Zhou 2010; Cha et al. 2016), and western North Pacific (WNP) monsoon region

**CONTACT** ZOU Liwei  zoulw@mail.iap.ac.cn

 Supplemental data for this article can be accessed [here](#).

© 2020 The Author(s). Published by Informa UK Limited, trading as Taylor & Francis Group.

This is an Open Access article distributed under the terms of the Creative Commons Attribution License (<http://creativecommons.org/licenses/by/4.0/>), which permits unrestricted use, distribution, and reproduction in any medium, provided the original work is properly cited.

(Zou and Zhou 2013). Comparison of global coupled ocean–atmosphere models and atmosphere-only models over the Asian monsoon region has also led to similar conclusions (Song and Zhou 2014).

The better performance of coupled global/regional models over the Asian monsoon region highlights the importance of local air–sea interactions. However, some studies argue that the improved climatology and inter-annual variability of monsoon precipitation and circulation in coupled models are largely due to compensation from SST biases that originate from atmospheric model biases (Song and Zhou 2014; Zou, Zhou, and Peng 2016; Yang et al. 2019). Indeed, the overall cold biases of the summer SST are found over the Asian monsoon region in both regional and global coupled models. These cold biases in global models are related to remote biases, i.e., the Atlantic Meridional Overturning Circulation (Wang et al. 2014) and tropical biases (Wang, Zou, and Zhou 2018), while those in regional coupled models are associated with regional biases (Li and Zhou 2010; Zou and Zhou 2011). The colder SSTs are, to some extent, responsible for the differences between the coupled and uncoupled global/regional models over the Asian monsoon region (Cha et al. 2016; Zou and Zhou 2016; Yang et al. 2019).

The Weather Research and Forecasting (WRF) model, which is a community regional climate model, has been widely used for regional climate studies over Asia (e.g., Liang et al. 2019). Version 4 of the WRF model (WRF4) has just been released, and so a comparison of ocean–atmosphere coupled versus atmosphere-only WRF4 models over the WNP is a necessary but as yet unreported line of investigation. In this study, we use a newly developed regional coupled ocean–atmosphere model based on WRF4 and the high-resolution regional version of LICOM (the State Key Laboratory of Numerical Modeling for Atmospheric Sciences and Geophysical Fluid Dynamics/Institute of Atmospheric Physics (LASG/IAP) Climate Ocean Model) to investigate the impacts of regional air–sea coupling on the simulation of the western North Pacific summer monsoon (WNPSM) through comparison with the corresponding stand-alone WRF4 model. The study focuses on 2005, which was a normal WNPSM year. The thermodynamic and dynamic effects of the warm biases of simulated SST on rainfall and circulation are revealed by conducting moisture and moist static energy budget analysis.

## 2. Models, experiments, and observational datasets

The regional coupled ocean–atmosphere model WRF4-LICOM is described in detail in Zou et al. (2020). Briefly,

the recently released WRF4 is used as the regional atmospheric model. The horizontal resolution of WRF4 is set to 15 km. The physics configuration is listed in the Supplementary Material. In this study, a North Pacific version of LICOM, named LICOM\_np (Yu, Liu, and Lin 2012), was employed as the oceanic model component. LICOM\_np was developed based on LICOM2 (Liu et al. 2012). The horizontal resolution of LICOM\_np is uniformly  $0.1^\circ$ .

The model domain of WRF4 was set to the WNP ( $5^\circ\text{S}$ – $45^\circ\text{N}$ ,  $100^\circ$ – $170^\circ\text{E}$ ). The coupled regional simulation with WRF4-LICOM started on 1 November 2004. Before that, LICOM\_np was spun up with the daily atmospheric forcing from CORE phase II from 2007. The coupling over the WNP region between WRF4 and LICOM\_np was performed hourly. The initial and lateral boundary conditions of WRF4 were derived from ERA-Interim (Dee et al. 2011), with a horizontal resolution of  $0.75^\circ \times 0.75^\circ$ . The boundary forcing data were updated every 6 h.

Both the coupled (WRF4-LICOM) and uncoupled (WRF4) regional models forced by the observed SSTs were integrated for year, from 1 November 2004 through 30 November 2005. The year 2005 was selected since it was a normal WNPSM year. To facilitate the following discussion, the coupled and uncoupled simulations are referred to as ‘WRF4\_CPL’ and ‘WRF4\_CTRL’, respectively. The satellite-retrieved and reanalysis data used to evaluate the models’ performances are listed in the Supplementary Material. For brevity, these data are simply referred to as ‘observation’.

## 3. Results

### 3.1. Rainfall and circulations

Figure 1 shows the spatial distributions of the rainfall, geopotential height of 5880 gpm, representing the western North Pacific subtropical high (WNPSH), and low-level wind at 850 hPa, averaged from June to August of 2005, derived from the observation and simulations. In the observation (Figure 1(a)), the major rainbands are found over the monsoon trough, the northern South China Sea, southern China, and the mei-yu front region from the Yangtze–Huai River Valley to the Korean Peninsula. In WRF4\_CTRL (Figure 1(b)), compared to the observation, followed by an overly strong and westward-shifted WNPSH, the simulated rainfall over the monsoon trough and southern China are underestimated, while those over the mei-yu front region are overestimated. The spatial correlation coefficient (SCC) of the rainfall between the observation and WRF4\_CTRL is 0.38.

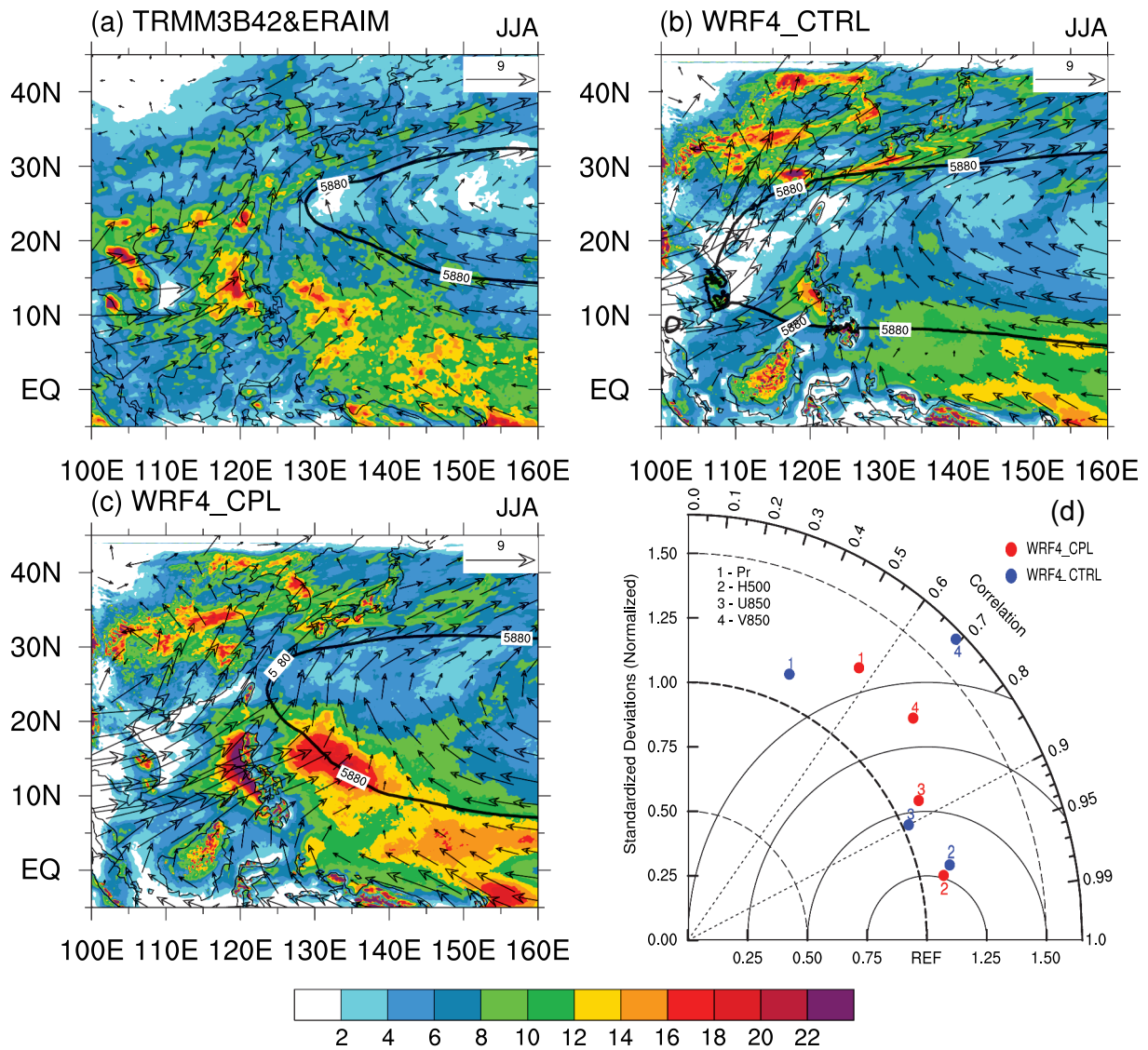


**Figure 1.** Spatial distributions of precipitation (shading; units:  $\text{mm d}^{-1}$ ), the 5880 gpm isoline at 500 hPa (contour), and the low-level wind at 850 hPa (vectors; units:  $\text{m s}^{-1}$ ) averaged from June to August 2005 over the WNP derived from (a) observation, (b) WRF4\_CTRL, and (c) WRF4\_CPL. (d) Taylor diagram evaluating the WRF4\_CTRL and WRF4\_CPL simulations of precipitation (Pr), geopotential height at 500 hPa ( $H500$ ), and horizontal ( $U850$ ) and meridional ( $V850$ ) winds at 850 hPa over the WNP. The angular coordinates are the correlation coefficients between the model results and the observations. The radial coordinate is the standard deviation of the model results divided by the standard deviation of the observations.

With the inclusion of regional air–sea coupling (Figure 1(c)), the strength and shape of the simulated WNPSH are improved compared to those of WRF4\_CTRL. The simulated rainfall (Figure 1(c)) over the monsoon trough and the northern South China Sea increase remarkably, and the dry biases over southern China in WRF4\_CTRL are alleviated. The spatial pattern of the simulated rainfall is improved in WRF4\_CPL, as evidenced by the higher SCC (0.56).

Figure 1(d) presents a Taylor diagram to quantitatively evaluate the models' performances in the

simulation of rainfall and circulation fields. The distance between each point and the point marked 'REF' on the horizontal axis is the root-mean-square error (RMSE). It is evident that WRF4\_CPL performs better than WRF4\_CTRL in the simulation of rainfall and most circulation variables over the WNP in terms of the SCC and RMSE, except for the meridional wind at 850 hPa.

With the inclusion of regional air–sea coupling, evident increases in rainfall are found over the northern South China Sea and east of the Philippines (Figure 2(a)), with a central value larger than  $13 \text{ mm d}^{-1}$ . The enhanced

heating associated with the increased rainfall simulates a low-level anomalous cyclone to its northwest due to a baroclinic Rossby wave response. The anomalous cyclone weakens the overly strong WNPSH simulated by WRF4\_CTRL.

To uncover why the rainfall increases over the northern South China Sea and east of the Philippines, a moisture budget analysis was performed with a focus on the region (10°–20°N, 115°–140°E). Based on the moisture budget equation and the continuity equation, the differences in rainfall between WRF4\_CPL and WRF4\_CTRL can be expressed as follows:

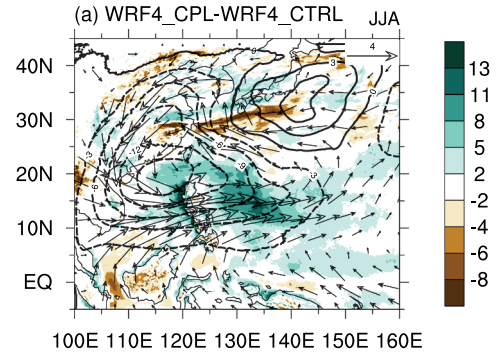
$$P' = E' - \langle \mathbf{V}_{\text{ctrl}} \cdot \mathbf{q}' \rangle - \langle u' \partial_x q_{\text{ctrl}} \rangle - \langle v' \partial_y q_{\text{ctrl}} \rangle - \langle \omega' \partial_p q_{\text{ctrl}} \rangle + \text{NL}' \quad (1)$$

where  $P$  is rainfall;  $E$  is evaporation;  $\mathbf{V}$  and  $q$  are the horizontal wind vector and specific humidity, respectively;  $u$ ,  $v$ , and  $\omega$  are the zonal wind, meridional wind, and vertical pressure-velocity, respectively; angle brackets, i.e.,  $\langle \rangle$ , represent column integration from the surface to 100 hPa; a prime ( $'$ ) denotes the difference between WRF4\_CPL and WRF4\_CTRL (WRF4\_CPL minus WRF4\_CTRL); and the subscript 'ctrl' denotes the WRF4\_CTRL simulation. According to Equation (1), the differences in simulated rainfall between WRF4\_CPL and WRF4\_CTRL can be attributed to changes in surface evaporation, moisture flux convergence contributed by changes in moisture only (thermodynamic term), moisture flux convergence associated with changes in zonal, meridional, and vertical velocity (dynamic term), and the nonlinear term (NL).

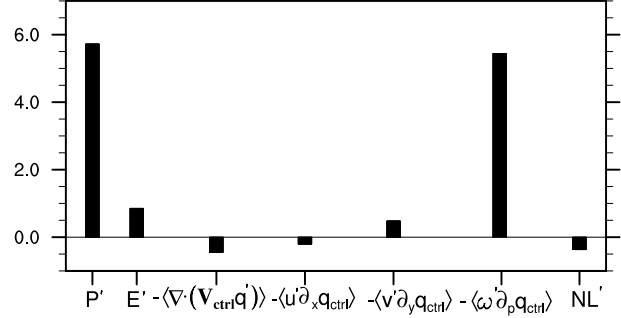
The analysis results (Figure 2(b)) indicate that a more than 90% increase in simulated rainfall over the region (10°–20°N, 115°–140°E) in the WRF4\_CPL can be attributed to the increased moisture vertical advection associated with the ascending anomalies ( $-\langle \omega' \partial_p q_{\text{ctrl}} \rangle$ ), i.e., the increased moisture convergence associated with the enhanced horizontal wind convergence. The second contributor is surface evaporation.

### 3.2. Moist static energy budget and SST bias

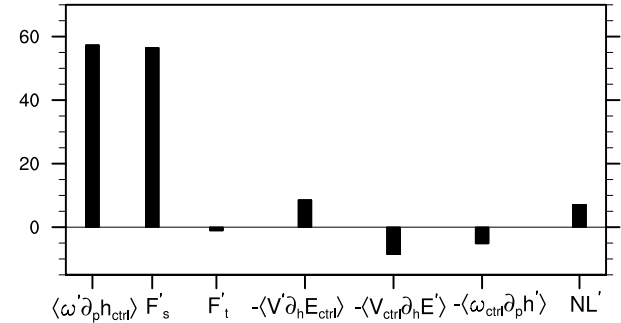
To further understand the ascending anomalies in WRF4\_CPL relative to those in WRF4\_CTRL over the region (10°–20°N, 115°–140°E), the moist static energy (MSE) budget is diagnosed, since the vertical motion is constrained by the MSE budget in the tropics (Neelin and Held 1987). Similar to the moisture budget equation, the MSE equation can be written as:



(a) WRF4\_CPL-WRF4\_CTRL JJA



(b) Moisture Budget



(c) Moist Static Energy Budget

**Figure 2.** (a) Differences in rainfall (shading; units:  $\text{mm d}^{-1}$ ) and wind vector at 850 hPa (vectors; units:  $\text{m s}^{-1}$ ) averaged from June to August of 2005 between WRF4\_CPL and WRF4\_CTRL (WRF4\_CPL minus WRF4\_CTRL). (b) Moisture processes responsible for rainfall differences over the region (10°–20°N, 115°–140°E) averaged from June to August of 2005 between WRF4\_CPL and WRF4\_CTRL (WRF4\_CPL minus WRF4\_CTRL). (c) Budget analysis of the moist static energy equation for the region (10°–20°N, 115°–140°E). See text for details.

$$\langle \omega' \partial_p h_{\text{ctrl}} \rangle = F'_s + F'_t - \langle \mathbf{V}_{\text{ctrl}} \cdot \mathbf{h} M' \rangle - \langle \mathbf{V}' \cdot \mathbf{h} M_{\text{ctrl}} \rangle - \langle \omega_{\text{ctrl}} \partial_p h' \rangle + \text{NL}' \quad (2)$$

where  $h$  is MSE,  $M$  is moist enthalpy,  $F_s$  is surface net heat flux (upward is positive), and  $F_t$  is net heat flux at the top of the atmosphere (downward is positive).

The analysis results (Figure 2(c)) indicate that the positive net surface heat flux  $F_s$  makes the largest contribution to the anomalous ascending motion. The second strongest contributor is the horizontal advection of the enthalpy by

**Table 1.** Observed and simulated net solar radiation (SR), long-wave radiation (LW), sensible heat (SH), and latent heat (LH) at the sea surface averaged from June to August 2005 for the region ( $10^{\circ}$ – $20^{\circ}$ N,  $115^{\circ}$ – $140^{\circ}$ E). The observed radiation fluxes (turbulence fluxes) are from CERES (OAFlux) data. Downward is positive for SR, while upward is positive for the other heat fluxes. Units:  $\text{W m}^{-2}$ .

	Observation	WRF4_CTRL	WRF4_CPL
SR	213.5	265.8	236.2
LW	46.4	52.6	48.9
SH	7.1	10.1	13.3
LH	114.4	115.8	143.2

anomalous wind ( $-\langle \mathbf{V}' \cdot \mathbf{h} M_{\text{ctrl}} \rangle$ ). The positive net surface heat flux is followed by reduced downward solar radiation at the sea surface and enhanced upward latent heat flux (Table 1). The former is associated with enhanced convection, while the latter is associated with positive SST

biases over the east of the Philippines (Figure 3(d)), which reduce the gross moist stability of the atmospheric column.

But what causes the warm SST biases in WRF4\_CPL? Note that weak warm SST biases are already found in the stand-alone LICOM model (Figure S1), while the coupling tends to further increase the warm biases. Compared to the observation (Figure 3(a)), the simulated surface net heat flux that heats the ocean is overestimated over the east of the Philippines in WRF4\_CTRL (Figure 3(b)), which implies a potential warm heat source. With the inclusion of regional air–sea coupling, this warm heat source favors warm SST biases over the east of the Philippines (Figure 3(d)). The simulated surface net heat flux is improved in WRF4\_CPL (Figure 3(c)).

The warmer SST may be the initial trigger. On the one hand it reduces the gross moist stability of the

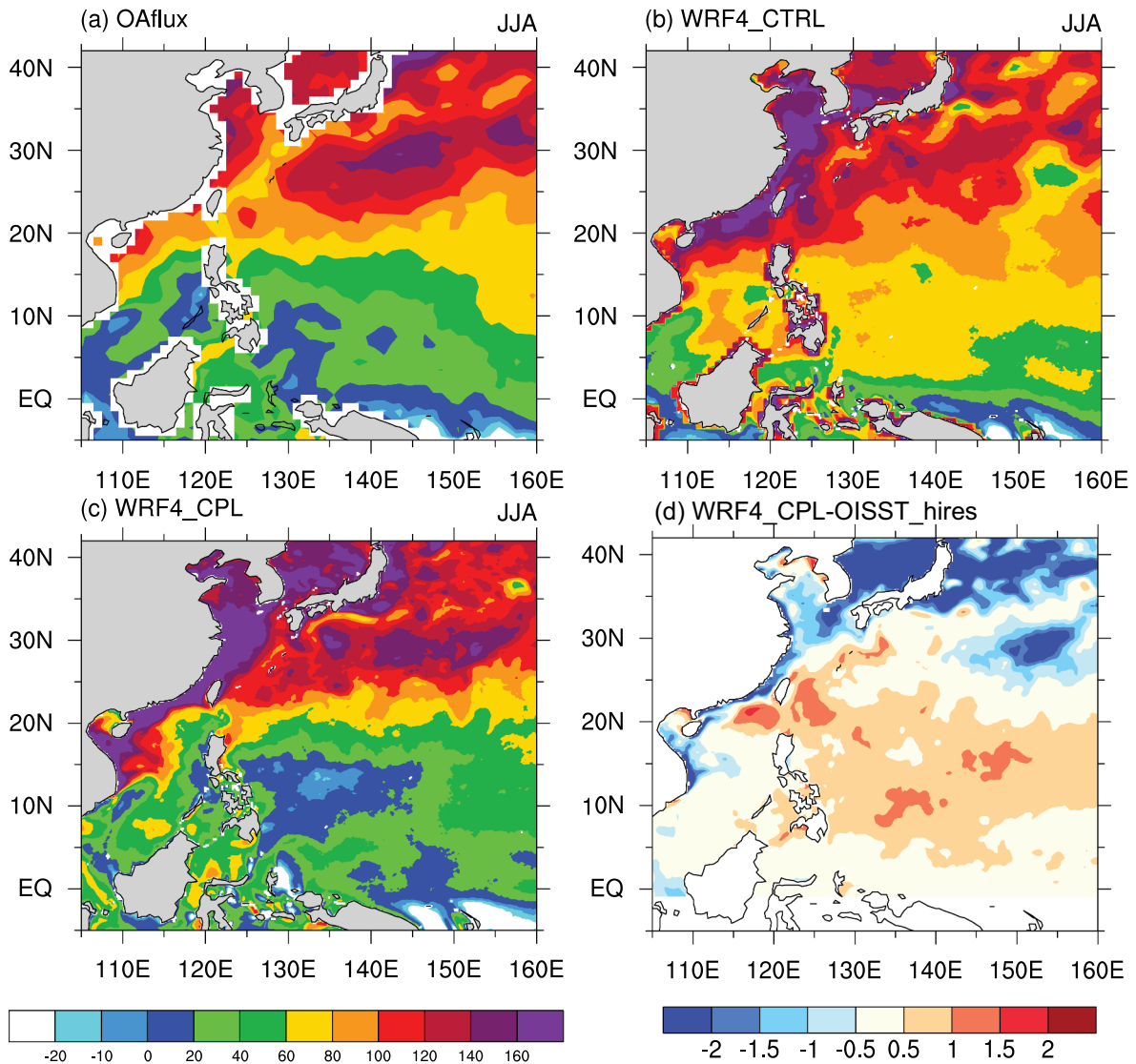


**Figure 3.** Spatial distributions of net sea surface heat fluxes (downward is positive; units:  $\text{W m}^{-2}$ ) averaged from June to August of 2005 derived from (a) observation, (b) WRF4\_CTRL, and (c) WRF\_CPL. (d) Spatial distributions of the simulated SST biases from WRF4\_CPL.

atmosphere and then increases the upward latent heat flux, which drives local ascending anomalies and then increases convective rainfall; whilst on the other hand, it changes the SST gradient and then increases the lower-level wind convergence, according to Lindzen and Nigam (1987). The resultant enhanced condensational heating drives a low-level anomalous cyclone to its northwest.

### 3.3. Daily variability

The inclusion of regional air–sea coupling also improves the simulation of the daily evolution of rainfall over the WNP. Figure S2 shows the latitudinal evolution of the rainfall band averaged between 105°E and 140°E from 1 May to 31 August 2005. In the observation, the northward propagation of the monsoon rainband starts from about 15°N in early June to about 35°N in early July and then retreats southwards to approximately 13°N in later July. The simulated rainband over the mei-yu front region is overestimated, and the northward jump of the rainband is hardly seen in WRF4\_CTRL (Figure S2). The northward movement of the rainband is partly reproduced by WRF4\_CPL, as evidenced by the SCC of 0.29 versus 0.21, although it is still not perfect (Figure S2).

But why does the inclusion of regional air–sea interactions improve the simulation of the summer monsoon over the WNP in WRF4? In the observation, the summer monsoon and its variability over the WNP are mainly driven by the large-scale thermal contrast. Therefore, the local SST over the WNP is actually a response to the overlying summer monsoon rather than a forcing to the atmosphere. The importance of air–sea coupling for the WNPSM is not only at the interannual time scale (Wang et al. 2005; Wu, Kirtman, and Pegion 2006; Wu and Kirtman 2007; Wu, Zhou, and Li 2009) but also at the intraseasonal time scale (Wu, Cao, and Chen 2018; Wu 2019). The observed daily SST anomalies over the region (10°–20°N, 115°–140°E) during 1 June to 31 August 2005 are negatively correlated with the local rainfall anomalies (Figure 4(a)), with a correlation of  $-0.29$ . Less (more) rainfall affected by remote forcing favors more (less) solar radiation reaching the sea surface, which leads to a warmer (colder) SST. The observed daily surface solar radiation is positively correlated with the local SST (Figure 4(d)), with a correlation of  $0.45$ .

The observed daily SST–rainfall and SST–surface solar radiation relationships over the region (10°–20°N, 115°–140°E) are poorly simulated in WRF4\_CTRL (Figure 4(b, e)). In WRF4\_CTRL, the observed SST and ‘remote forcing’ are already prescribed as the lower and lateral boundary conditions, respectively. Since the regional air–sea coupling is not included, the modeled

atmosphere exhibits a strong response to the underlying daily SST anomalies. The simulated daily rainfall anomalies are positively correlated with the local SST (Figure 4(b)), with a correlation of  $0.37$ . Warmer (colder) SST increases (decreases) the local rainfall, and then leads to less (more) solar radiation reaching the sea surface (Figure 4(e)), as evidenced by the negative correlation of  $-0.35$ .

In WRF4\_CPL, with the inclusion of regional air–sea coupling, compared to WRF4\_CTRL, the relationship between the rainfall and the local SST over the region (10°–20°N, 115°–140°E) is improved, with a correlation of  $-0.30$  (Figure 4(c)). The dry biases in WRF4 lead to more solar radiation reaching the sea surface and thereby warm the SST. The warmer SST tends to reduce the dry biases. Therefore, the relationship between the SST and surface solar radiation is also improved, with a correlation of  $0.46$ . These results highlight the importance of regional air–sea coupling in the simulation of the summer monsoon and its variability over the WNP.

## 4. Summary

In this study, a new coupled ocean–atmosphere regional model, WRF4-LICOM, developed by LASG/IAP, was used to investigate the impacts of regional air–sea coupling on the simulation of the WNPSM. Coupled and uncoupled regional simulations were compared with a focus on the normal WNPSM year 2005. The main results can be summarized as follows:

- (1) Compared to the atmosphere-only WRF4 model, the coupled regional model (WRF4-LICOM) improved the simulation of summer mean monsoon rainfall and circulations in terms of both SCC and RMSE. The simulated biases in the stand-alone WRF4, including the dry biases over the monsoon trough and southern China and the overly strong WNPSH, were significantly reduced in WRF4-LICOM. More than 90% of the increased rainfall over the northern South China Sea and east of the Philippines in the WRF4\_CPL could be attributed to the increased moisture vertical advection associated with the ascending anomalies.
- (2) Warm biases of the simulated SST were found over the central WNP region in WRF4-LICOM. The biases were triggered by the overestimated downward sea surface net heat flux simulated by the atmosphere-only WRF4 model. The positive SST biases tended to increase the surface evaporation and decrease the solar radiation reaching the sea surface, leading to improved simulation of the surface net heat flux.

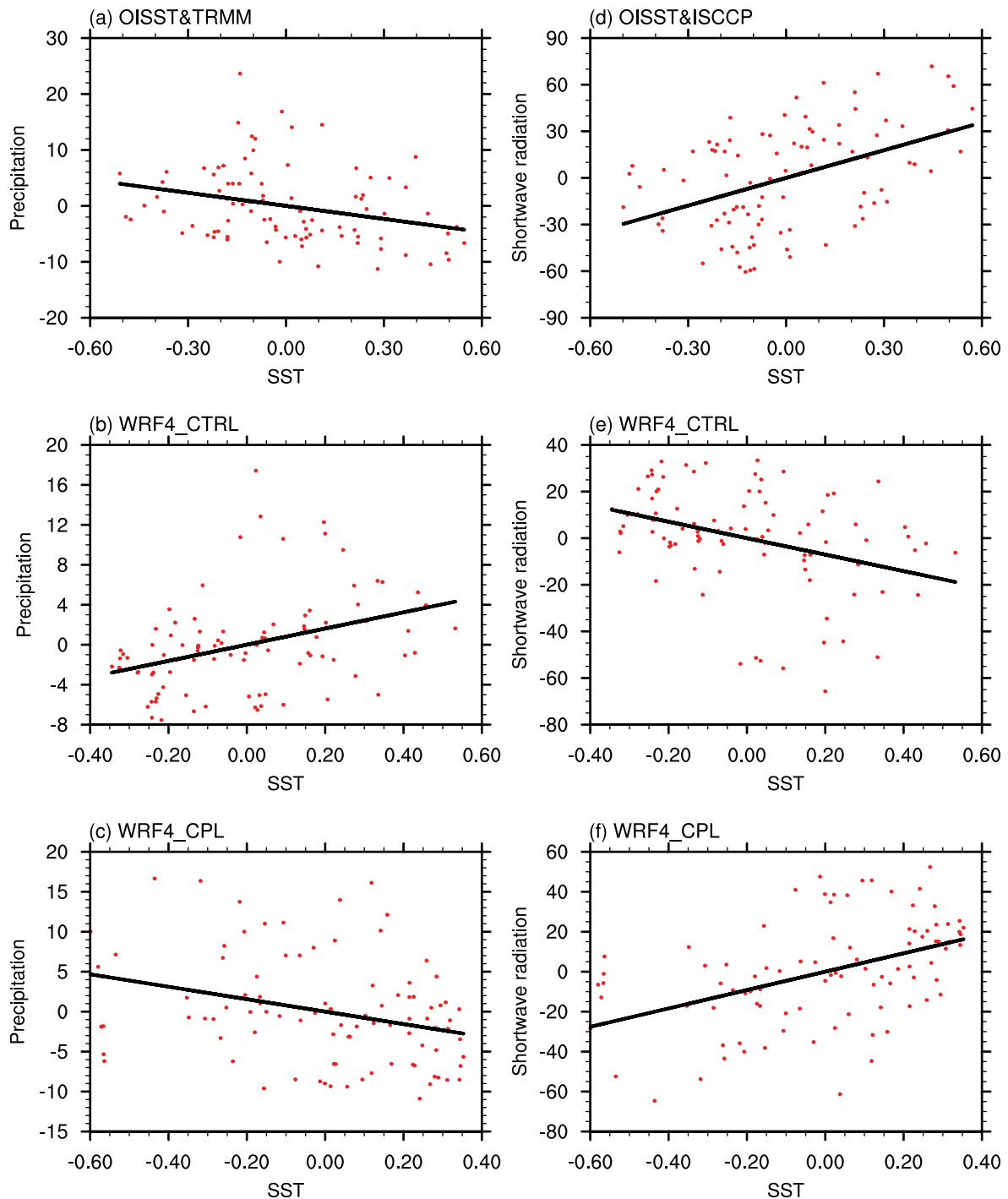


**Figure 4.** (a–c) Scatterplots of the regional-averaged daily SST (units:  $^{\circ}\text{C}$ ) and precipitation (units:  $\text{mm d}^{-1}$ ) anomalies over the region ( $10^{\circ}$ – $20^{\circ}\text{N}$ ,  $115^{\circ}$ – $140^{\circ}\text{E}$ ) from 1 June to 31 August 2005 from (a) observation, (b) WRF4\_CTRL, and (c) WRF4\_CPL. (d–f) Scatterplots of the regional-averaged SST (units:  $^{\circ}\text{C}$ ) and sea surface net shortwave radiation (units:  $\text{W m}^{-2}$ ) from (d) observation, (e) WRF4\_CTRL, and (f) WRF4\_CPL. The monthly means of rainfall, SST, and sea surface net shortwave radiation have been removed from the original data.

(3) The warmer SST reduced the gross moist stability of the atmosphere and increased the upward latent heat flux, which drove local ascending anomalies and then increased the convective rainfall in WRF4-LICOM. The resultant enhanced atmospheric heating drove a low-level anomalous

cyclone to its northwest, which tended to reduce the simulated circulation biases in the stand-alone WRF4 model.

(4) The observed SST–rainfall and SST–surface solar radiation relationships over the central WNP region were poorly simulated in the stand-alone



WRF4 model. The modeled atmosphere in the stand-alone WRF4 model exhibited a strong response to the underlying daily SST anomalies. In WRF4-LICOM, the inclusion of regional air–sea coupling tended to improve the simulations of daily SST–rainfall and SST–surface solar radiation relationships, highlighting the importance of regional air–sea coupling in the simulation of the summer monsoon and its variability over the WNP.

The focus of this study was on a normal WNPSM year (2005) by conducting a one-year simulation. A previous study indicated that the inclusion of regional air–sea coupling improved the simulation of the interannual variability of the WNPSM in a regional climate model (Zou and Zhou 2013). Whether WRF4-LICOM performs better than the stand-alone WRF4 model in simulating the interannual variability of the WNPSM deserves further investigation. In addition, there are hundreds of ways in which the physics can be configured in WRF4. The improvements from regional air–sea coupling may depend on the selected physics configuration. This dependence will be investigated in the future.

## Acknowledgments

The comments from the two anonymous reviewers are greatly appreciated.

## Disclosure statement

No potential conflict of interest was reported by the author.

## Funding

This work was jointly supported by the National Natural Science Foundation of China [grant number 41875132] and The National Key Research and Development Program of China [grant number 2018YFA0606003].

## References

- Cha, D.-H., C. S. Jin, J. H. Moon, and D. K. Lee. 2016. "Improvement of Regional Climate Simulation of East Asian Summer Monsoon by Coupled Air–sea Interaction and Large-scale Nudging." *International Journal of Climatology* 36: 334–345. doi:10.1002/joc.4349.
- Dee, D. P., S. M. Uppala, A. J. Simmons, P. Berrisford, P. Poli, S. Kobayashi, U. Andrae, et al. 2011. "The ERA-Interim Reanalysis: Configuration and Performance of the Data Assimilation System." *Quarterly Journal of Royal Meteorological Society* 137: 553–597. doi:10.1002/qj.828.
- Giorgi, F. 2019. "Thirty Years of Regional Climate Modeling: Where are We and Where are We Going Next?" *Journal of Geophysical Research-Atmosphere* 124: 5696–5723. doi:10.1029/2018JD030094.
- Gutowski, J. W., F. Giorgi, B. Timbal, A. Frigon, D. Jacob, H.-S. Kang, K. Raghavan, et al. 2016. "WCRP COordinated Regional Downscaling EXperiment (CORDEX): A Diagnostic MIP for CMIP6." *Geoscientific Model Development* 9: 4087–4095. doi:10.5194/gmd-9-4087-2016.
- Hagos, S. M., and K. H. Cook. 2009. "Development of a Coupled Regional Model and Its Application to the Study of Interactions between the West African Monsoon and the Eastern Tropical Atlantic Ocean." *Journal of Climate* 22 (10): 2591–2604. doi:10.1175/2008JCLI2466.1.
- Li, T., and G. Zhou. 2010. "Preliminary Results of a Regional Air–sea Coupled Model over East Asia." *Chinese Science Bulletin* 55: 2295–2305. doi:10.1007/s11434-010-3071-1.
- Liang, X.-Z., C. Sun, X. Zheng, Y. Dai, M. Xu, H. I. Choi, T. Ling, et al. 2019. "CWRF Performance at Downscaling China Climate Characteristics." *Climate Dynamics* 52: 2159–2184. doi:10.1007/s00382-018-4257-5.
- Lindzen, R. S., and S. Nigam. 1987. "On the Role of Sea Surface Temperature Gradients in Forcing Low-level Winds and Convergence in the Tropics." *Journal of Atmospheric Sciences* 44: 2418–2436. doi:10.1175/1520-0469(1987)044<2418:OTROSS>2.0.CO;2.
- Liu, H., P. Lin, Y. Yu, and X. Zhang. 2012. "The Baseline Evaluation of LASG/IAP Climate System Ocean Model (LICOM) Version 2." *Acta Meteorologica Sinica* 26: 318–329. doi:10.1007/s13351-012-0305-y.
- Neelin, J. D., and I. M. Held. 1987. "Modeling Tropical Convergence Based on the Moist Static Energy Budget." *Monthly Weather Review* 115: 3–12. doi:10.1175/1520-0493(1987)115<0003:MTCBOT>2.0.CO;2.
- Ratnam, J. V., F. Giorgi, A. Kagainalkar, and S. Cozzini. 2009. "Simulation of the Indian monsoon using the RegCM3–ROMS regional coupled model." *Climate Dynamics* 33: 119–139. doi:10.1007/s00382-008-0433-3.
- Ren, X., and Y. Qian. 2005. "A Coupled Regional Air–sea Model, Its Performance and Climate Drift in Simulation of the East Asian Summer Monsoon in 1998." *International Journal of Climatology* 25: 679–692. doi:10.1002/joc.1137.
- Ruti, P. M., S. Somot, F. Giorgi, C. Dubois, E. Flaounas, A. Obermann, A. Dell'Aquila, et al. 2016. "Med-CORDEX Initiative for Mediterranean Climate Studies." *Bulletin of the American Meteorological Society* 97: 1187–1208. doi:10.1175/bams-d-14-00176.1.
- Song, F., and T. Zhou. 2014. "The Climatology and Interannual Variability of East Asian Summer Monsoon in CMIP5 Coupled Models: Does Air–sea Coupling Improve the Simulations?" *Journal of Climate* 27: 8761–8777. doi:10.1175/JCLI-D-14-00396.1.
- Wang, B., Q. Ding, X. Fu, I. S. Kang, K. Jin, J. Shukla, and F. Doblas-Reyes. 2005. "Fundamental Challenge in Simulation and Prediction of Summer Monsoon Rainfall." *Geophysical Research Letters* 32: L15711. doi:10.1029/2005GL022734.
- Wang, C., L. Zou, and T. Zhou. 2018. "SST Biases over the Northwest Pacific and Possible Causes in CMIP5 Models." *Science China Earth Sciences* 61: 792–803. doi:10.1007/s11430-017-9171-8.
- Wang, C. Z., L. Zhang, S. K. Lee, L. Wu, and C. R. Mechoso. 2014. "A Global Perspective on CMIP5 Climate Model Biases." *Nature Climate Change* 4: 201–205. doi:10.1038/nclimate2118.

- Wu, B., T.-J. Zhou, and T. Li. 2009. "Contrast of rainfall–SST Relationships in the Western North Pacific between the ENSO Developing and Decaying Summers." *Journal of Climate* 16: 4398–4405. doi:10.1175/2009JCLI2648.1.
- Wu, R. 2019. "Summer precipitation–SST Relationship on Different Time Scales in the Northern Tropical Indian Ocean and Western Pacific." *Climate Dynamics* 52 (9–10): 5911–5926. doi:10.1007/s00382-018-4487-6.
- Wu, R., and B. P. Kirtman. 2007. "Regimes of Local Air–sea Interactions and Implications for Performance of Forced Simulations." *Climate Dynamics* 29 (4): 393–410. doi:10.1007/s00382-007-0246-9.
- Wu, R., B. P. Kirtman, and K. Pegion. 2006. "Local Air–sea Relationship in Observations and Model Simulations." *Journal of Climate* 19 (19): 4914–4932. doi:10.1175/JCLI3904.1.
- Wu, R., X. Cao, and Z. Chen. 2018. "Relationship of Intraseasonal Variations of Atmosphere and Ocean in the South China Sea and Tropical Western North Pacific." *Chinese Journal of Atmospheric Sciences* 42 (4): 707–728. doi: 10.3878/j.issn.1006-9895.1712.17210. (In Chinese)
- Yang, B., Y. Zhang, Y. Qian, F. Song, L. R. Leung, P. Wu, Z. Guo, et al. 2019. "Better Monsoon Precipitation in Coupled Climate Models Due to Bias Compensation." *NPJ Climate and Atmospheric Science* 2: 43. doi:10.1038/s41612-019-0100-x
- Yu, Y., H. Liu, and P. Lin. 2012. "A Quasi-global 1/10° Eddy-resolving Ocean General Circulation Model and Its Preliminary Results." *Chinese Science Bulletin* 57: 3908–3916. doi:10.1007/s11434-012-5234-8.
- Zou, L., and T. Zhou. 2011. "Sensitivity of a Regional Ocean–atmosphere Coupled Model to Convection Parameterization over Western North Pacific." *Journal of Geophysical Research–Atmosphere* 116: D18106. doi:10.1029/2011JD015844.
- Zou, L., and T. Zhou. 2012. "A Review of Development and Application of Regional Ocean–atmosphere Coupled Model (In Chinese)." *Advances in Earth Science* 27 (8): 857–865.
- Zou, L., and T. Zhou. 2013. "Can a Regional Ocean Atmosphere Coupled Model Improve the Simulation of the Interannual Variability of the Western North Pacific Summer Monsoon?" *Journal of Climate* 26: 2353–2367. doi:10.1175/JCLI-D-11-00722.1.
- Zou, L., and T. Zhou. 2016. "A Regional Ocean–atmosphere Coupled Model Developed for CORDEX East Asia: Assessment of Asian Summer Monsoon Simulation." *Climate Dynamics* 47: 3627–3640. doi:10.1007/s00382-016-3032-8.
- Zou, L., T. Zhou, and D. Peng. 2016. "Dynamical Downscaling of Historical Climate over CORDEX East Asia Domain: A Comparison of Regional Ocean Atmosphere Coupled Model to Standalone RCM Simulations." *Journal of Geophysical Research–Atmosphere* 121: 1442–1458. doi:10.1002/2015JD023912.
- Zou, L., T. Zhou, H. Liu, and J. Tang. 2020. "Introduction to the Regional Coupled Model WRF4-LICOM: Performance and Model Intercomparison over the Western North Pacific." *Advances in Atmospheric Sciences* 37: 800–816. doi:10.1007/s00376-020-9268-6.